



Title	Abnormal Metal Bond Distances in PtAu Alloy Nanoparticles : In Situ Back-Illumination XAFS Investigations of the Structure of PtAu Nanoparticles on a Flat HOPG Substrate Prepared by Arc Plasma Deposition
Author(s)	Hu, Bing; Bharate, Bapurao; Jimenez, Juan D.; Lauterbach, Jochen; Todoroki, Naoto; Wadayama, Toshimasa; Higashi, Kotaro; Uruga, Tomoya; Iwasawa, Yasuhiro; Ariga-Miwa, Hiroko; Takakusagi, Satoru; Asakura, Kiyotaka
Citation	Journal of physical chemistry c, 126(2), 1006-1016 <a href="https://doi.org/10.1021/acs.jpcc.1c08393">https://doi.org/10.1021/acs.jpcc.1c08393</a>
Issue Date	2022-01-20
Doc URL	<a href="http://hdl.handle.net/2115/87843">http://hdl.handle.net/2115/87843</a>
Rights	This document is the Accepted Manuscript version of a Published Work that appeared in final form in The Journal of Physical Chemistry C, copyright c American Chemical Society after peer review and technical editing by the publisher. To access the final edited and published work see <a href="https://pubs.acs.org/articlesonrequest/AOR-NGNDHYXZEXYQKJEQXWZF">https://pubs.acs.org/articlesonrequest/AOR-NGNDHYXZEXYQKJEQXWZF</a> .
Type	article (author version)
Additional Information	There are other files related to this item in HUSCAP. Check the above URL.
File Information	jp1c08393_si_001.pdf (Supporting Information)



[Instructions for use](#)

## **Supplementary Information for:**

### **Abnormal Metal Bond Distances in PtAu Alloy Nanoparticles: *In situ***

#### **Back-Illumination XAFS Investigations of the Structure of PtAu**

#### **Nanoparticles on a Flat HOPG Substrate Prepared by Arc Plasma**

#### **Deposition**

Bing Hu,<sup>†</sup> Bapurao Bharate,<sup>†</sup> Juan D. Jimenez,<sup>‡</sup> Jochen Lauterbach,<sup>‡</sup> Naoto Todoroki,<sup>§</sup> Toshimasa Wadayama,<sup>§</sup> Kotaro Higashi,<sup>¶</sup> Tomoya Uruga,<sup>¶</sup> Yasuhiro Iwasawa,<sup>¶</sup> Hiroko Ariga-Miwa,<sup>¶</sup> Satoru Takakusagi<sup>†</sup>, Kiyotaka Asakura<sup>†\*</sup>

<sup>†</sup>Institute for Catalysis, Hokkaido University, Hokkaido 001-0021, Japan

<sup>‡</sup>Department of Chemical Engineering, University of South Carolina, 541 Main St., Columbia, SC 29208, USA

<sup>§</sup>Graduate School of Environmental Studies, Tohoku University, Sendai 980-8579, Japan

<sup>¶</sup>Innovation Research Center for Fuel Cells, University of Electro-Communications, Chofu, Tokyo 182-8585, Japan

<sup>‡</sup>Japan Synchrotron Radiation Research Institute (JASRI), Hyogo 679-5148, Japan

- 1. Experimental details**
- 2. XPS results**
- 3. CV and its analysis details**
- 4. EXAFS and its analysis details**
- 5. Change of the edge height.**
- 6. XANES of Pt L<sub>3</sub> and Au L<sub>3</sub> measured by BCLA+BI-XAFS**
- 7. Edge height of Pt<sub>10</sub>Au<sub>90</sub> foil**
- 8. Error estimation using  $\chi^2$  test**
- 9. HERFD-XANES by FEFF8**
- 10. Table about edge height dependence on potential**
- 11. Text-1 Details in BCLA+BI-XAFS experiment set up and XAFS analysis**
- 12. Text-2 Quantification of Pt in PtAu/HOPG by XPS**
- 13. Text-3 Deriving the error bar for the parameters in EXAFS fitting**
- 14. Text-4 Discerning the O-adsorption site from HERFD-XANES**

## Supplementary Figures

### 1. Experimental details

Sample transfer box.

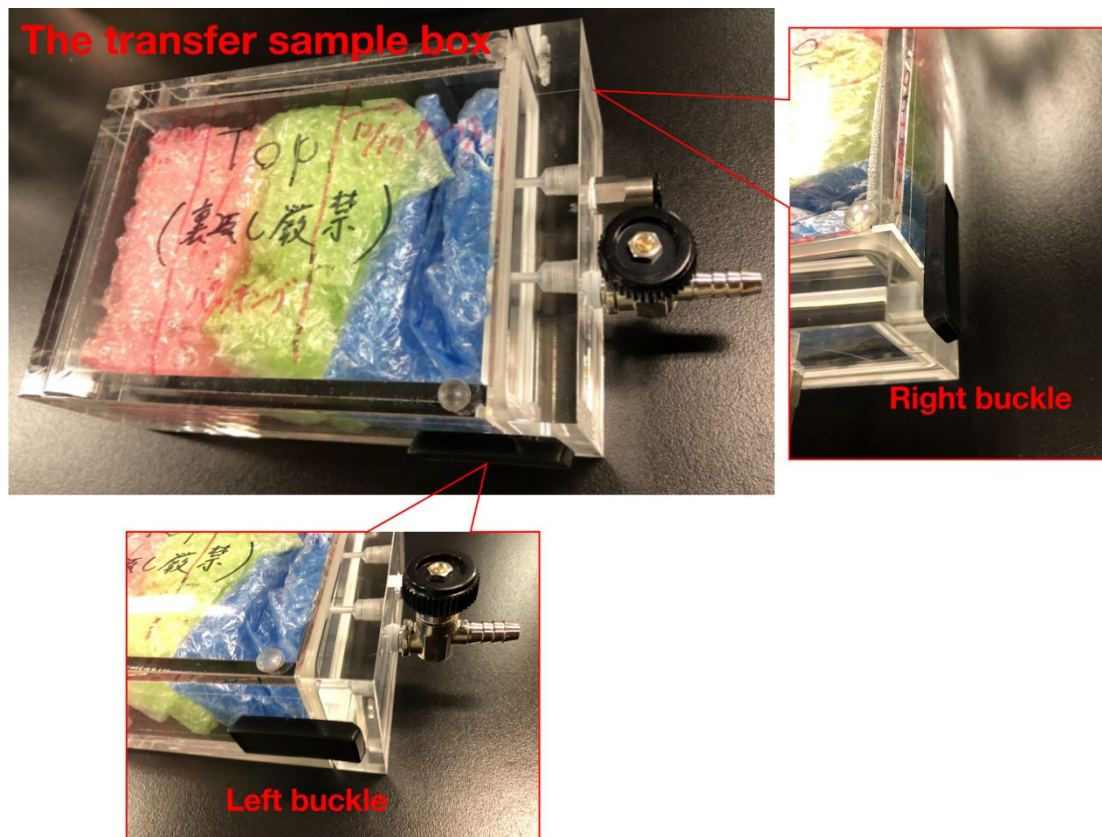


**Figure S1** The transfer sample box for keeping and transferring as-prepared PtAu/HOPG samples. At the first time, the inside of the box was replaced with Ar. Then, it was sent into the glove box to transfer samples. After that, the box was only opened in N<sub>2</sub> or Ar-filled glovebox, avoiding the exposure of the sample to the air.

The home-made electrochemical cell for in situ XAFS measurement and setup.

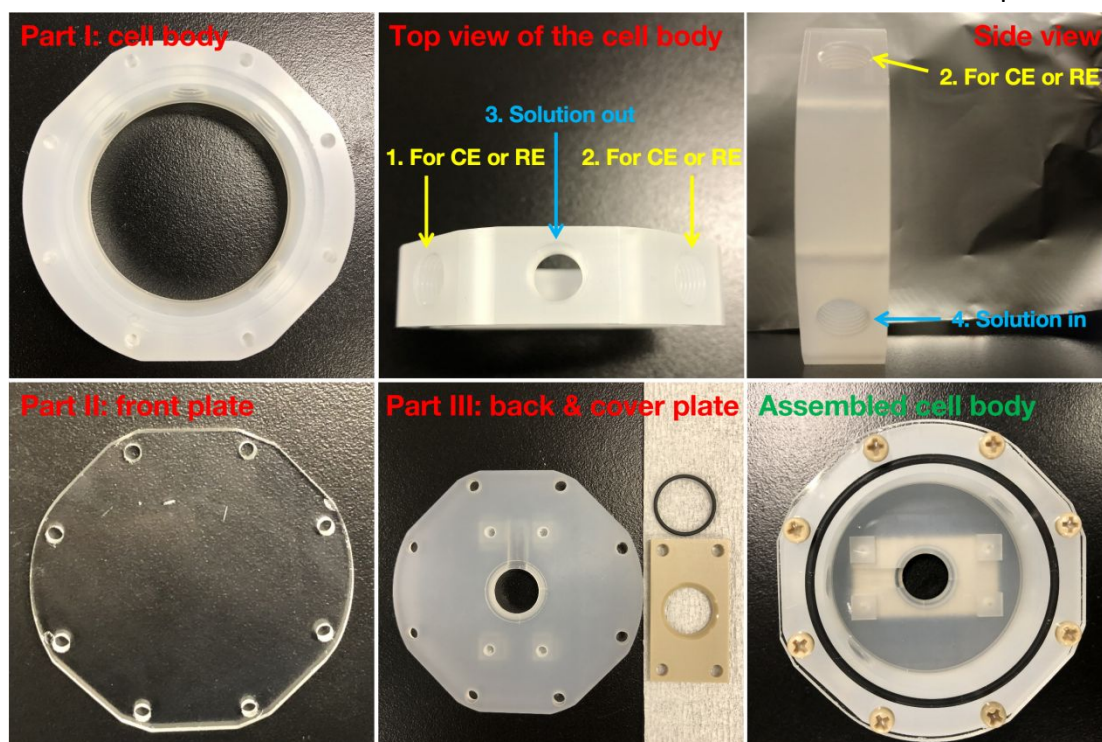


**Figure S2** The home-made electrochemical cell for in situ XAFS measurement. The upper three images show the cylindrical cell body with the four bolt holes designed for inserting the counter and reference electrode holders, the electrolyte inlet tube, and the electrolyte outlet tube. The different parts of the cell are joined by screws and the O-rings prevent the leakage of electrolyte and the infiltration of air.

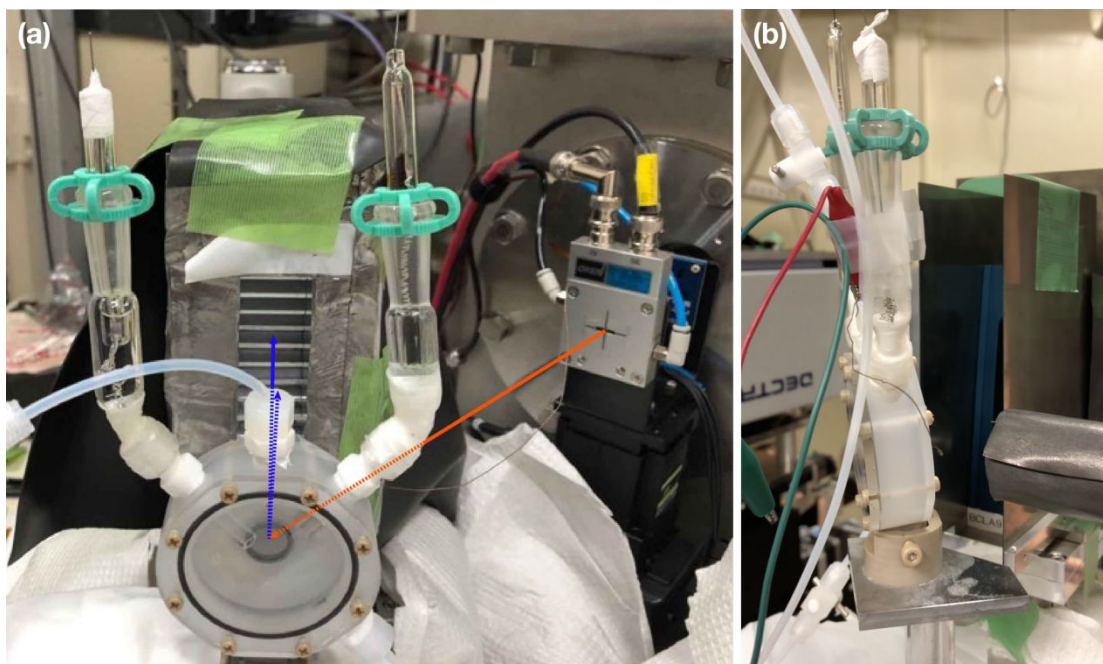


**Figure S3** (a) The in situ XAFS cell setup. (b) The BCLA + BI-XAFS setup under working. The red arrow in (a) depicts the incident X-ray and the blue arrows stand for the fluorescence that will be selected by the BCLA frames. (b) shows the copper wire connected to the red clip that conducts the electrochemical current from the backside of the PtAu/HOPG sample.

## 2. XPS results

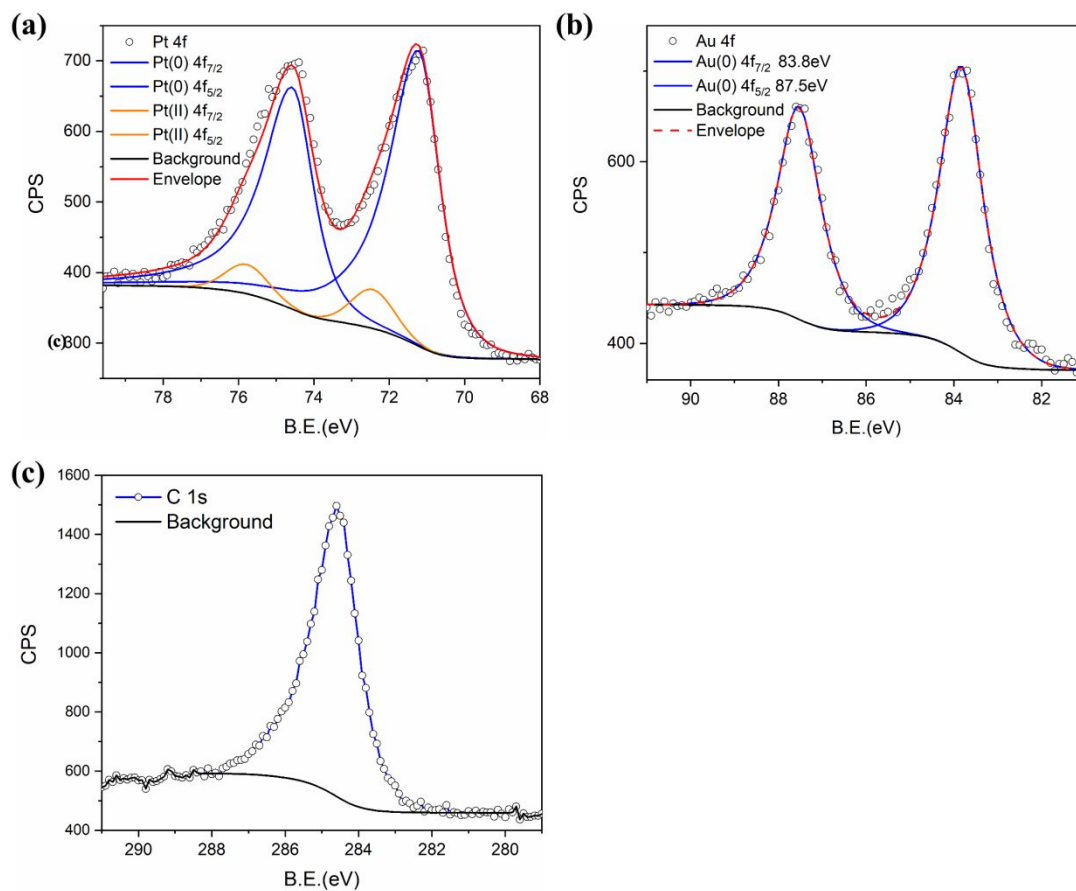


**Figure S4** XPS spectra of the PtAu/HOPG model surface. (a) Pt 4f spectra showed minor extent of Pt oxidation due to the exposure of the PtAu/HOPG sample to the air. (b) Au 4f spectra showed the stable metallic phase. (c) C1s spectra.



### 3. CV and its analysis details

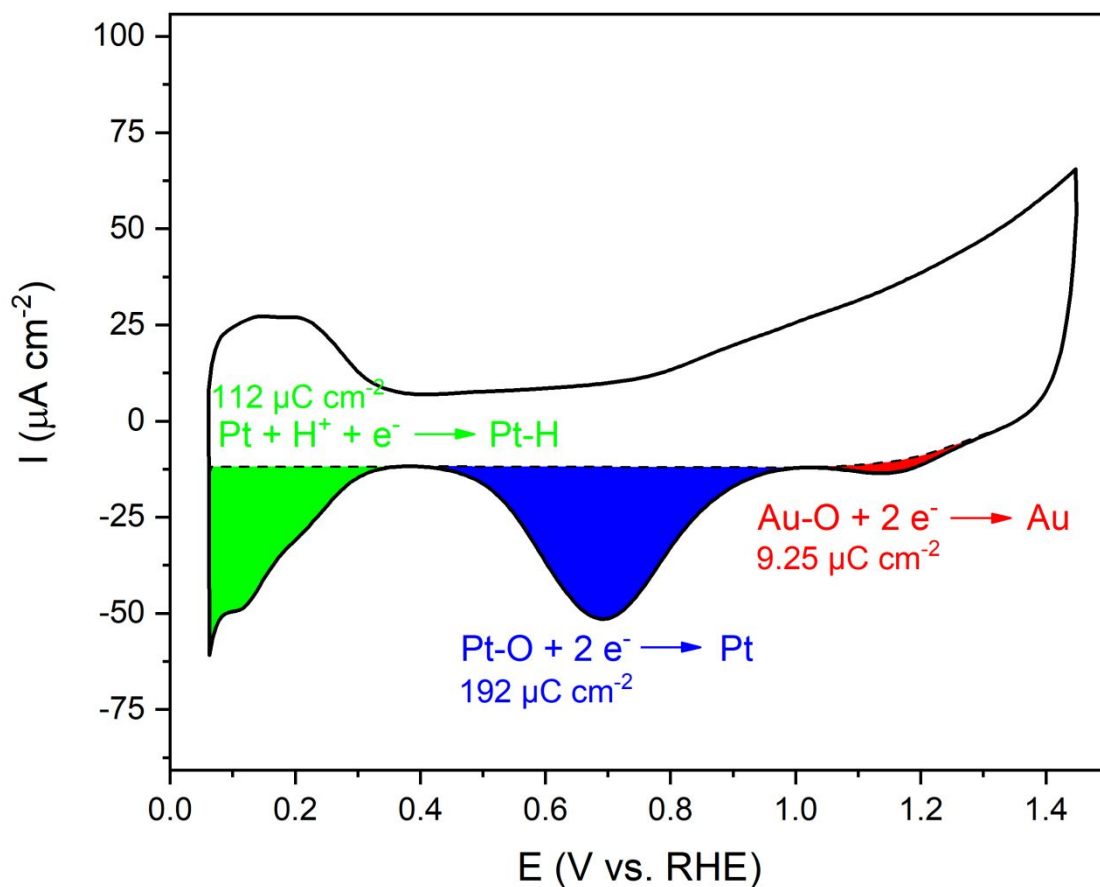


**Figure S5** Integration of the characteristic cathodic reduction peaks in the CV of PtAu/HOPG in 0.1 M HClO<sub>4</sub> with a scan rate of 50 mV s<sup>-1</sup>. The hydrogen underpotential deposition was from 0.37 V to 0.06 V and the baseline was double-layer current. Straight baselines were used for the integration of Pt-O reduction peak at 0.7 V and Au-O reduction peak at 1.2 V. As the electrochemical reduction process took place at the surface of PtAu nanoparticles (NPs), the ratio of surface Pt to Au was equal to the ratio of peak area, which was 21 : 1, indicating a Pt-dominant surface structure for the PtAu nanoparticles in PtAu/HOPG.

#### 4. EXAFS and its analysis details

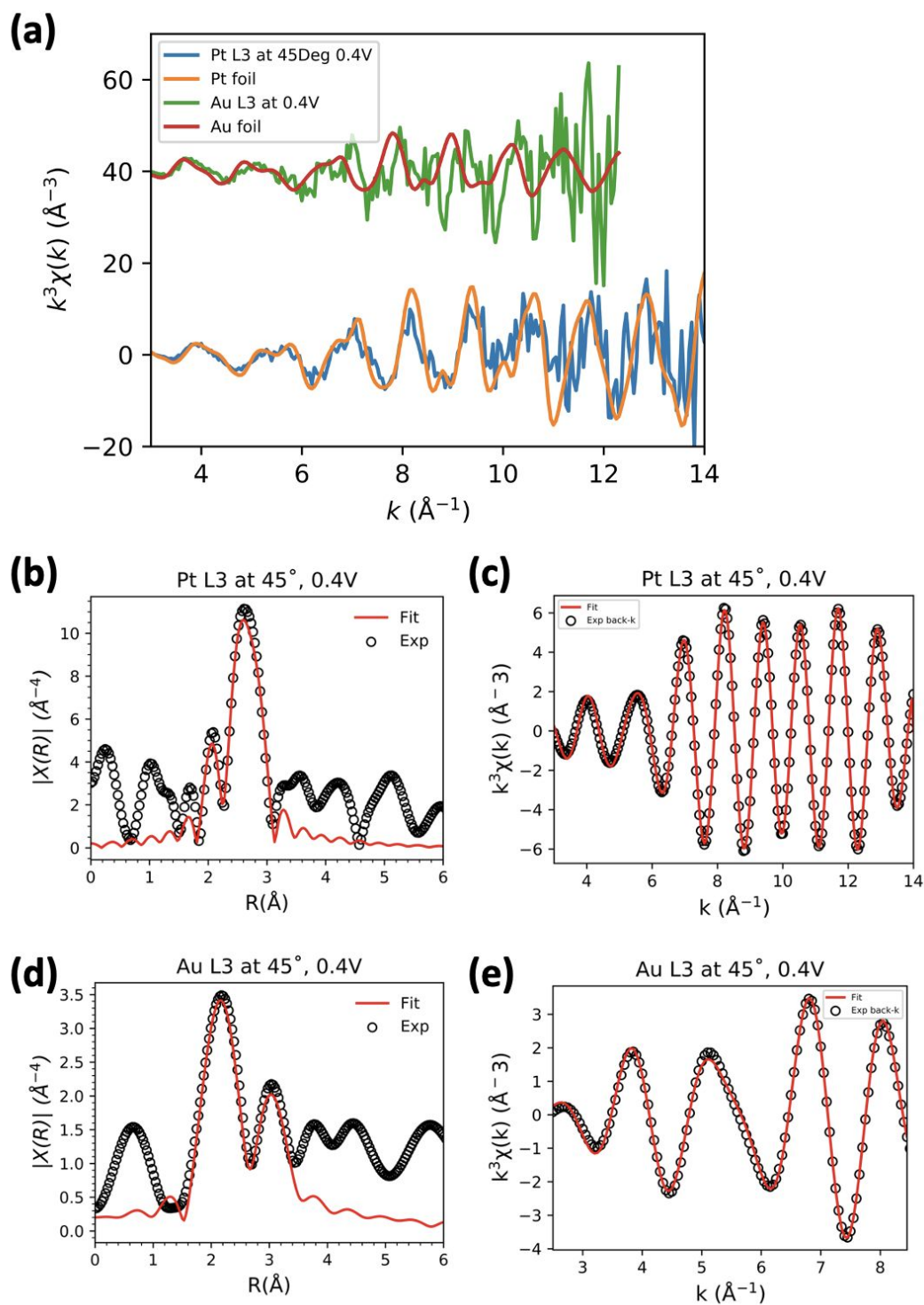


**Figure S6** (a) A comparison of the Pt L<sub>3</sub> and Au L<sub>3</sub>  $k^3\chi(k)$  spectra of PtAu/HOPG at 0.4  $V_{\text{RHE}}$  with those of Pt and Au foils. The FT data and inversely Fourier transformed data were superimposed with the fitting curves for (b, c) Pt L<sub>3</sub> and (d, e) Au L<sub>3</sub> at 0.4  $V_{\text{RHE}}$ . The  $k$ -range for FT was 3.0 – 14.0  $\text{\AA}^{-1}$  for Pt L<sub>3</sub> (c) and 2.5 – 8.5  $\text{\AA}^{-1}$  for Au L<sub>3</sub> (e). The  $R$ -range for back- $k$  fitting was 1.8 – 3.1  $\text{\AA}$  for Pt L<sub>3</sub> (b) and 1.6 – 3.4  $\text{\AA}$  for Au L<sub>3</sub> (d).



## 5. Change of the edge height.

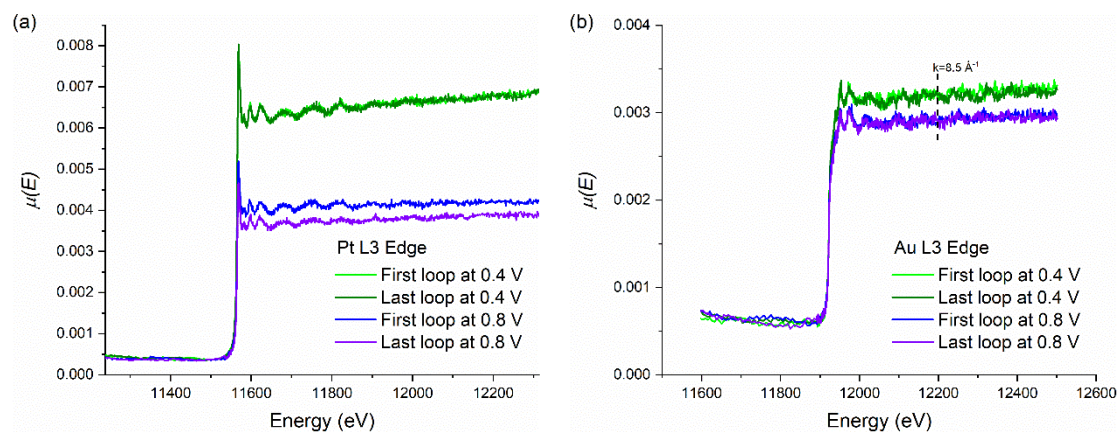


**Figure S7** Raw XAFS spectra of PtAu/HOPG for the first loop and the last loop under 0.4 V<sub>RHE</sub> and 0.8 V<sub>RHE</sub> at the Pt L<sub>3</sub> edge (a) and Au L<sub>3</sub> edge (b).

## 6. XANES of Pt L<sub>3</sub> and Au L<sub>3</sub> measured by BCLA+BI-XAFS

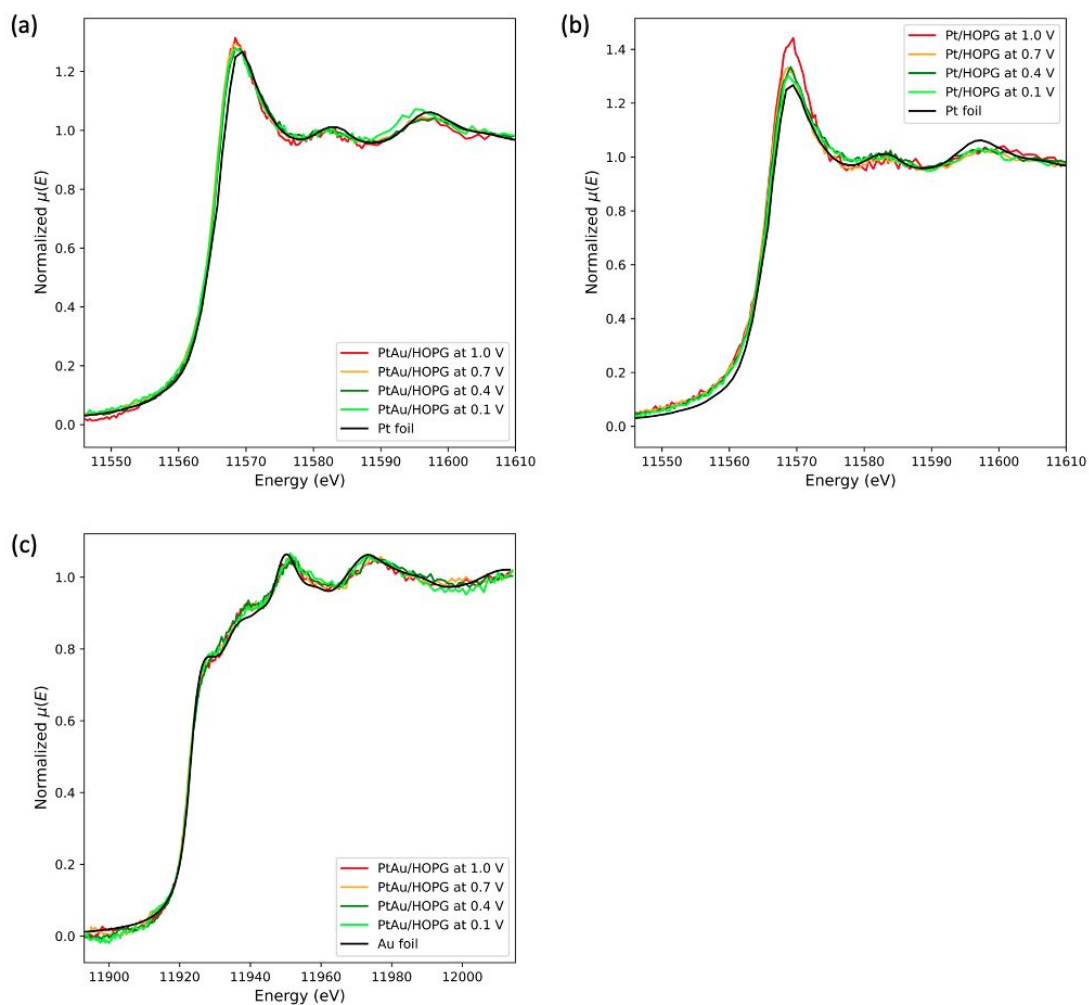


**Figure S8** XANES region of the Pt L<sub>3</sub> edge and Au L<sub>3</sub> edge measured at different electrode potentials by the BCLA-BI-XAFS method. (a) and (b) correspond to the Pt L<sub>3</sub> edge XANES of PtAu/HOPG and Pt/HOPG at various electrode potentials. (c) corresponds to the Au L<sub>3</sub> XANES spectra at different electrode potentials.

## 7. Edge height of Pt<sub>10</sub>Au<sub>90</sub> foil

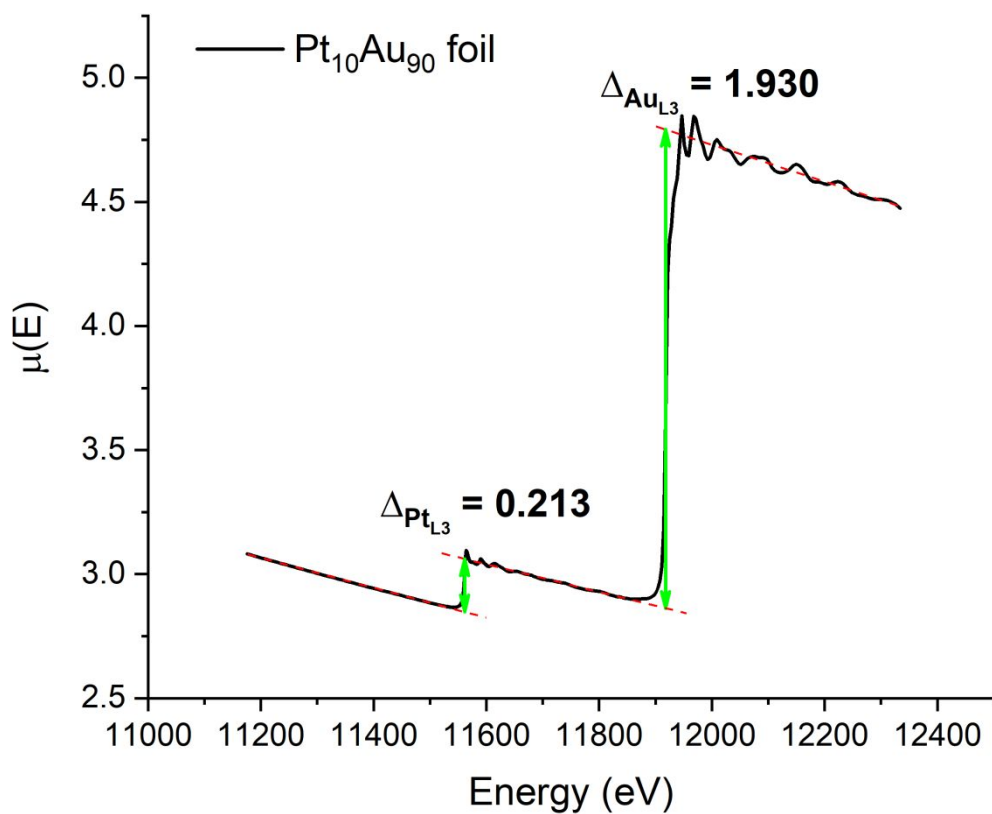


**Figure S9** Pt L<sub>3</sub> and Au L<sub>3</sub> XAFS of a Pt<sub>10</sub>Au<sub>90</sub> foil in transmission mode. The Pt L<sub>3</sub> and Au L<sub>3</sub> edge step ratio is 9.06, highly commensurate with the designated Pt : Au ratio of 9.

## 8. Error estimation using $\chi^2$ test

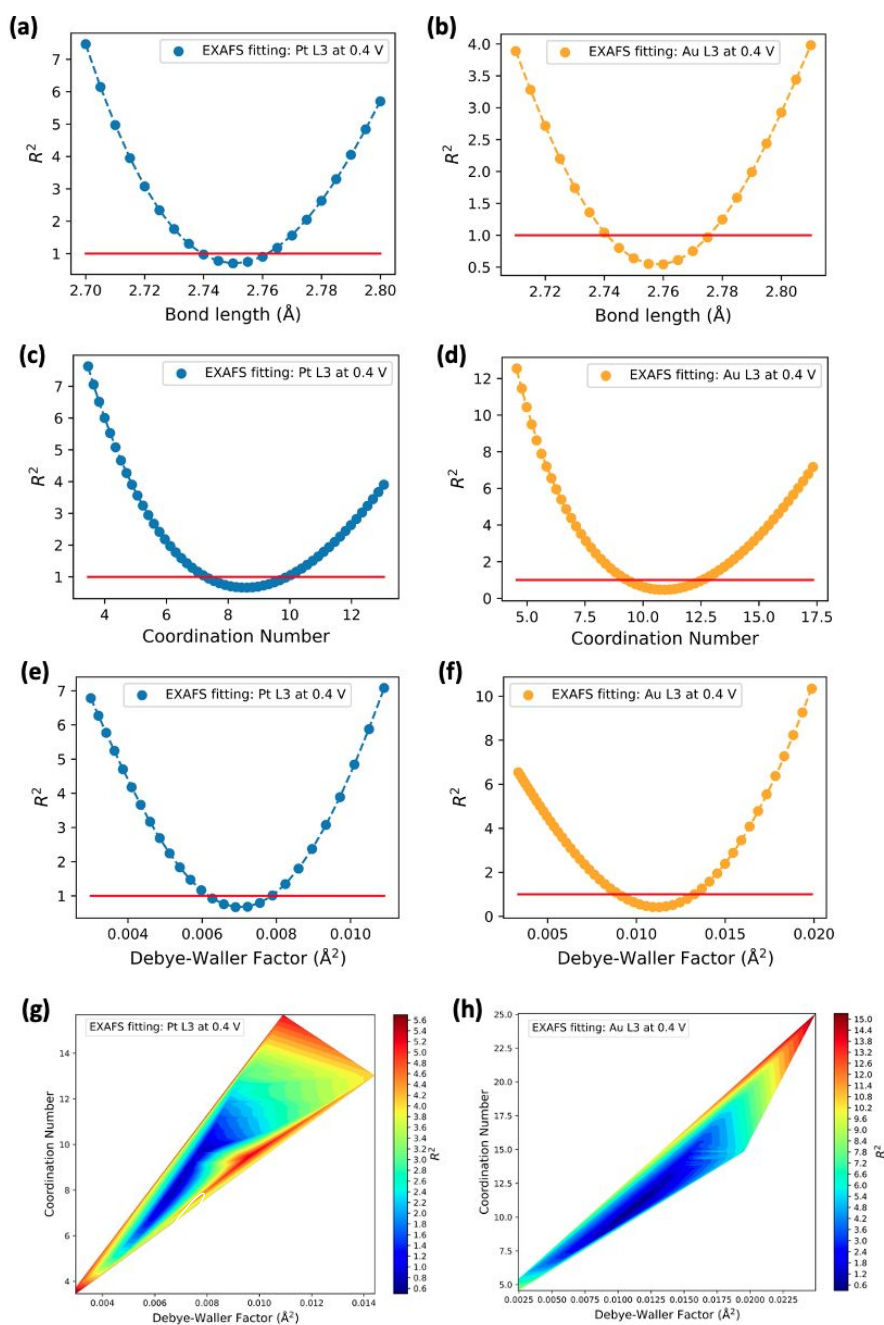


**Figure S10** The variation of the reduced R-factor, i.e.  $R^2$  (defined in SI-13 Text-3), of EXAFS fitting with the corresponding parameters. (a), (c), and (e) show the change of  $R^2$  with bond length, coordination number, and Debye-Waller Factor for the 0.4 V Pt L<sub>3</sub> edge EXAFS fitting, respectively. Similarly, (b), (d), and (f) show those of 0.4 V Au L<sub>3</sub> edge EXAFS fitting. (g) and (h) are the contour plots of Coordination number and Debye Waller factor. The dashed line serves as the guide for the eye for  $\chi^2$ -test. The solid red line marks the threshold, so that  $R^2$  larger than 1 were rejected. (g) and (f) are the contour map to show the correlation between coordination number and Debye-Waller factor. The white oval indicates the region of  $R^2 < 1$

## 9. HERFD-XANES by FEFF8

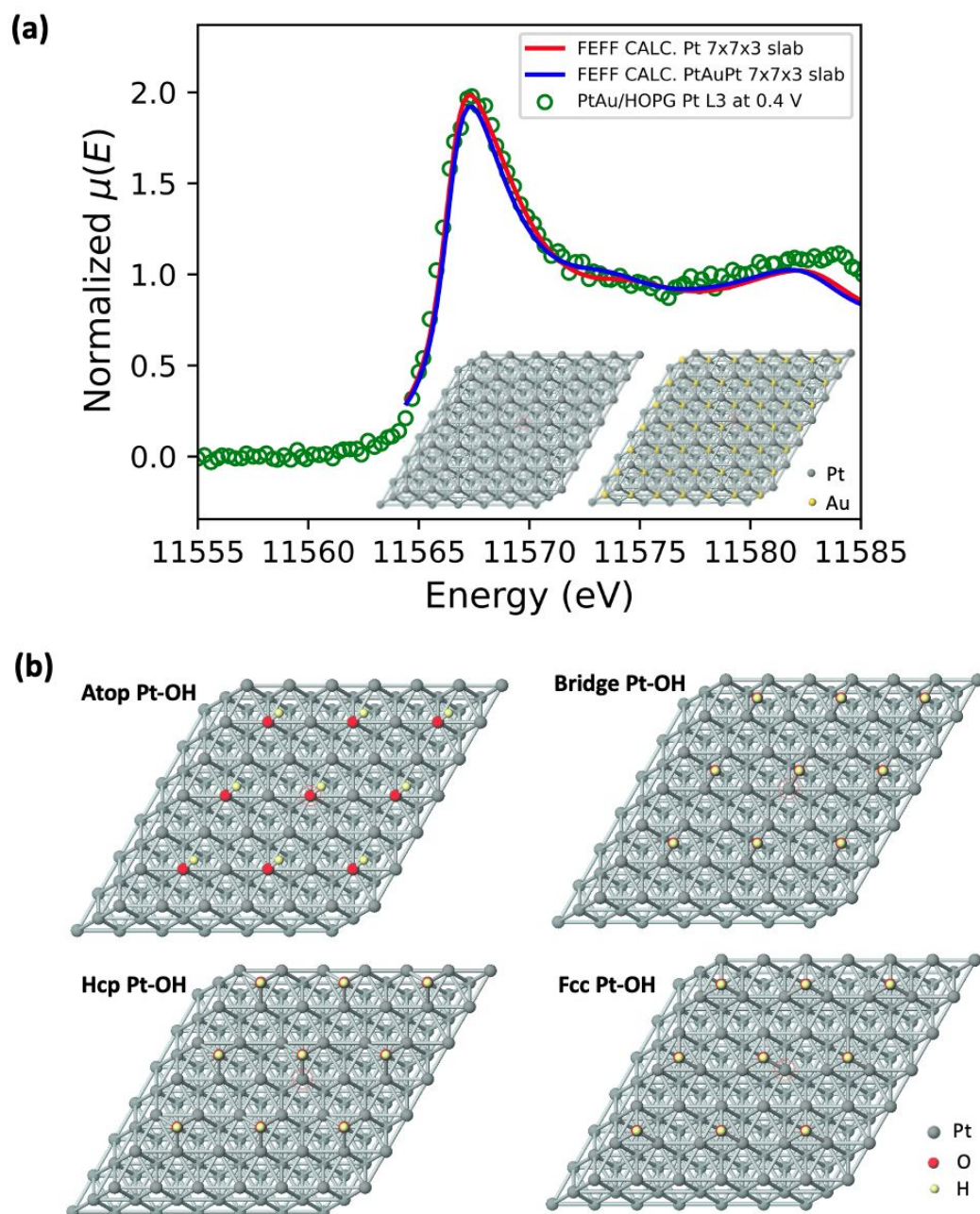


**Figure S11** (a) FEFF – calculated Pt  $L_3$  XANES spectra of the Pt  $7 \times 7 \times 3$  (111) (red curve) and PtAuPt  $7 \times 7 \times 3$  (111) slab (blue curve) (bond length =  $2.75 \text{ \AA}$ ) compared with the HERFD-XANES Pt  $L_3$  spectra of PtAu/HOPG measured at 0.4 V. (b) 4 types of adsorption site models on Pt  $7 \times 7 \times 3$  (111) for FEFF simulations.

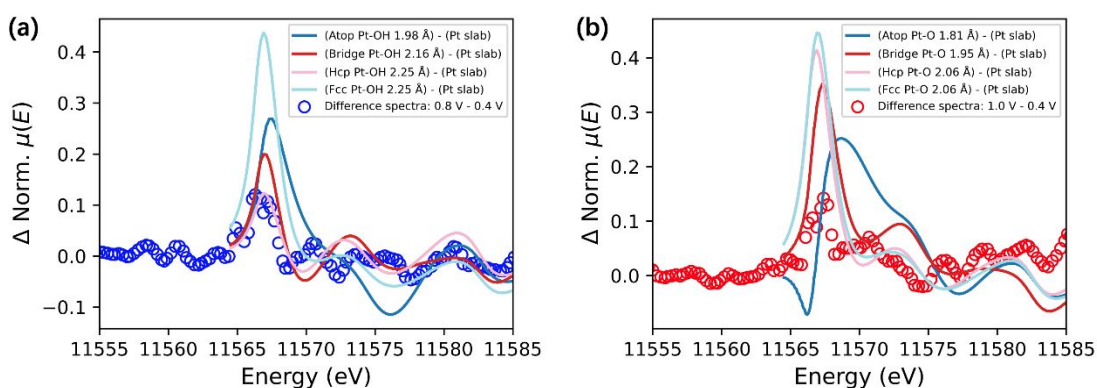


**Figure S12** Comparison of the experimental HERFD-XANES difference spectra with the calculated difference spectra. (a) The blue circles are the difference spectra of Pt  $L_3$  HERFD-XANES of PtAu/HOPG at 0.8 V subtracted by that at 0.4 V. The colored lines are the calculated difference spectra derived from the FEFF calculation for OH-adsorbed Pt subtracted by that of Pt on Pt  $7 \times 7 \times 3$  slab. The slight shift towards lower energy was reproduced by the Hcp( or Fcc) site. (b)The red circles are the difference spectra of the Pt  $L_3$  HERFD-XANES of PtAu/HOPG at 1.0 V subtracted by that at 0.4 V. The colored lines are the calculated difference spectra derived from the FEFF calculation for O-adsorbed Pt subtracted by that of Pt on Pt  $7 \times 7 \times 3$  slab. The feature of higher energy shift and peak broadening in Figure 5d is qualitatively reproduced by the adsorption on the Bridge site.



## Supplementary Table

### 10. Table about edge height dependence on potential

**Table S1** The edge steps of Pt and Au measured at corresponding conditions, from which the atomic composition of Pt and Au in the NPs can be deduced as shown in the last column. Selective dissolution of Pt can be observed.

Potential (V)	Pt L <sub>3</sub> edge step	Au L <sub>3</sub> edge step	Pt/Au ratio
0.4	0.0058	0.0026	2.3
0.5	0.0053	0.0025	2.1
0.7	0.0051	0.0023	2.2
0.8	0.0035	0.0023	1.6
0.9	0.0028	0.0023	1.2
1.0	0.0020	0.0023	0.9
0.4 <sup>a</sup>	0.0076	0.0033	2.3

<sup>a</sup> After 1.0 V<sub>RHE</sub>, the electrode potential was returned to 0.4 V<sub>RHE</sub> and the sample was shifted so that the irradiated position was shifted by a few millimeters (mm).

## Supplementary Texts

### 11. Text-1: Details in BCLA+BI-XAFS experiment set up and XAFS analysis

#### (A) Details in BCLA+BI-XAFS experiment set up

Figure S2 shows a polychlorotrifluoroethylene (PCTFE) cylindrical cell body, a glass plate, and a PCTFE back plate. Four holes were drilled in the side surface of the PCTFE cylindrical cell body. Two holes were for a reference electrode and a counter electrode, the other two were for the inlet and outlet of the electrolyte. The back plate had a  $\varnothing$  12 mm hole for the HOPG window, which was ringed with a  $\varnothing$  15 mm groove for the O-ring seal. The HOPG window was pressed to the O-ring by the rectangular cover plate with the screws to seal the cell. The HOPG window front side with the PtAu nanoparticle deposited was directed inwards the cell contacting the electrolyte. Between the rectangular cover plate and the backside of HOPG a copper plate was inserted and was welded to a copper wire to collect the current from the PtAu/HOPG working electrode. In this way, the HOPG served as an electrode, a substrate, and an X-ray window. During XAFS measurement, the incident and fluorescence X-rays went through the thin HOPG window. Figure S3 shows photos of the sample cell setup under the working conditions. Each Pt  $L\alpha$  or Au  $L\alpha$  fluorescent X-ray was selected by the BCLA from the other and the undesired scattering X-ray. The selection of fluorescence lines could be made by adjusting the position of BCLA. The monochromatized fluorescence was collected by the 25-element Ge solid state detector (SSD) as illustrated in Figure 1.

#### (B) EXAFS analysis

The edge-step was defined as the difference between the values of the interpolated post-edge and pre-edge lines at the absorption edge,  $E_0$ . For XANES normalization, the “Least-square 1<sup>st</sup>” background method was used for deriving the pre-edge background and the normalization point was chosen to be at the middle of the peaks and troughs of the oscillations. For EXAFS fitting analysis, the “Least-square 1<sup>st</sup>” background method was adopted for pre-edge background generation and the “Cook-Sayers Spline-smoothing” method for the post-edge  $\mu_0$ -background in a way that minimized the removal of main oscillation from the raw data. After background removal, the raw EXAFS spectra were normalized into the oscillatory  $\chi(k)$  spectra, where  $k$  was the photoelectron wavenumber transformed from the incident X-ray energy ( $E$ ) via following equation:

$$k = \sqrt{\frac{2m_e(E - E_0)}{\hbar^2}} \quad (S1)$$

where  $E_0$  was the absorption edge determined as the maximum in the 1<sup>st</sup> derivative of the edge jump. The  $k^3\chi(k)$  data were Fourier transformed (FT) and then the first-shell of the FT spectra was inversely transformed into  $k$ -space, which was fitted via the EXAFS equation:

$$k^3\chi(k) = S_0^2 \sum_i k^3 \frac{N_i F_i(k, R_i)}{k R_i^2} \sin(2kR_i + \psi_i(k, R_i)) e^{\frac{-2R_i}{\lambda_i(k)}} e^{-2\sigma_i^2 k^2} \quad (S2)$$

$S_0^2$  was the amplitude reduction factor which was determined using Pt foil or Au foil  $L_3$  edge data.  $F_i(k, R_i)$ ,  $\psi_i(k, R_i)$ , and  $\lambda(k)$  were the  $i$ -th shell scattering amplitude, phase shift, and inelastic mean free path calculated in FEFF 8 from Pt or Au face centered cubic clusters. Fitting parameters were  $N_i$ ,  $R_i$ , and  $\sigma_i^2$ , namely the  $i$ -th shell coordination number (CN), bond length, and Debye-Waller (DW) factor. Since the scattering amplitude and phase shifts of Pt and Au were almost the same, we performed a single shell fitting for the EXAFS data.

## 12. Text-2: Quantification of Pt in PtAu/HOPG by XPS

We were particularly concerned about the quantity of Pt (as well as Au) deposited on the HOPG surface. For the Pt(111) surface with Pt-Pt bond length of 2.78 Å, the Pt number density was  $1.49 \times 10^{15} \text{ cm}^{-2}$ , defined as 1 monolayer (ML). The reason that the amount of Pt should be controlled at about 1 ML was to realize the idea of “well-defined” surface, which was corresponding to be less than a single layer of nanoparticles on the HOPG surface. Less than 1ML of the Pt concentration on the model surface was not enough to acquire high-quality XAFS spectra. Consequently the 1 ML loading was the most appropriate one.

The ratio of Pt:Au deposited onto the HOPG surface was 2.5 : 1 as determined by the 4f photoelectron spectra of Pt and Au (Figure S4). The HOPG surface was composed of atomically flat layers of carbon honeycombs with C-C bond length of 1.42 Å and inter-layer distance of 3.35 Å, corresponding to  $3.8 \times 10^{15}$  carbon atoms per  $\text{cm}^2$ . As XPS was measured with Mg  $K\alpha$  source of energy 1253.6 eV, the kinetic energy of C 1s photoelectron was 970 eV, giving a mean free path of about 3 nm in carbonaceous materials.<sup>1</sup> Because the loading of Pt was about 1 ML or 0.2 nm, we neglected PtAu overlayer and assumed that the C 1s photoelectron from the PtAu/HOPG sample only damped due to C layers. Based on the mean free path and graphitic interlayer distance, the total C 1s signal was 8.2 times that of a monolayer of carbon, as calculated based on the equation below:

$$N = N_0 e^{-\frac{D}{\lambda \sin\theta}} \quad (\text{S3})$$

( $N$  was the number of  $C_{1s}$  photoelectrons detected that were originated from the source C atoms with a depth of  $D$  from the HOPG surface.  $\theta$  was angle between the exiting path of the photoelectron and the HOPG surface, which was  $90^\circ$  in this work.  $\lambda$  was the mean free path of the photoelectron.)

Given the photoionization cross section of Pt  $4f_{7/2}$  and C 1s subshells to be 8.7 and 1, the XPS provided the density of surface Pt to be  $2.0 \times 10^{15} \text{ cm}^{-2}$  or the coverage to be 1.4 ML.

### 13. Text-3: Deriving the error bar for the parameters in EXAFS fitting

The uncertainties in the fitting parameters were determined using the  $\chi^2$  test as described by Eq. S4:

$$R^2 = \frac{M}{(M - \nu)N} \sum_k \frac{|\chi_{obs}(k) - \chi_{cal}(k)|^2}{\varepsilon(k)^2} \quad (S4)$$

where N was the number of data points for EXAFS fitting;  $\chi_{obs}(k)$  and  $\chi_{cal}(k)$  were the experimental and calculated ones;  $\varepsilon(k)$  was the statistical error in the experimental spectrum. M was the number of information ( $=2 \Delta k \Delta r/\pi + 2$ ) and  $\nu$  was the number of fitting parameters. The goodness of fit was evaluated by  $R^2$  such that when  $R^2$  was smaller than 1 the fit was adopted. The errors in the fitting parameters were estimated as shown in Figure S10. In order to show the correlation between coordination number and Debye Waller factor, we made contour plots in Figure S10. The white oval shape shows  $R^2 < 1$  and we did not find the large correlation between them.

### 14. Text-4: Discerning the O-adsorption site from HERFD-XANES

The subtle changes in HERFD-XANES spectra under different potentials is considered to be induced by the surface adsorbates of -H, -OH, -O. We carried out the FEFF calculation to interpret the difference of HERFD-XANES spectra.

We calculated the XANES spectra of the central Pt atom on the surfaces of the 7x7 Pt (111) 3 layer slab (denoted as Pt 7 × 7 × 3) and the 7x7 Pt/Au/Pt (111) 3 layer slab (denoted as PtAuPt 7 × 7 × 3) by FEFF. The imaginary part of EXCHANGE card is set at -1.7 to reduce the core life time so as to reproduce the sharpening of the white line peak.<sup>2</sup> From Figure S11a, it can be seen that FEFF-calculated XANES of both Pt 7 × 7 × 3 and PtAuPt 7 × 7 × 3 rather well reproduced the HERFD-XANES spectra of PtAu/HOPG measured at 0.4 V.

We investigated the adsorption of -OH and -O on the Pt of Pt 7 × 7 × 3 surfaces for simplicity at 4 types of sites, namely Atop, Bridge, Hcp, and Fcc, as shown in Figure S11b. The bond length was referenced from the work by Han et al.<sup>3</sup> in each of the -OH and -O adsorbed models, which were used to represent the cases of 0.8 V<sub>RHE</sub> and 1.0 V<sub>RHE</sub>, respectively. Figure S12a shows the difference spectra between Pt L<sub>3</sub>-edge HERFD XANES at 0.8 V<sub>RHE</sub> and at 0.4 V<sub>RHE</sub> together with those calculated from FEFF based on the four adsorption sites. The slight shift towards lower energy was reproduced by the Hcp (or Fcc) site. The change at 1.0 V<sub>RHE</sub> experimental spectra (Figure 5d) could be reproduced by the adsorption on the Bridge site (Figure S12b). We tentatively conclude that -OH is adsorbed at 0.8 V on the Hcp(or Fcc) site while at 1.0 V -O is adsorbed on the Bridge site, though further studies including the calculations of PtAu nanoparticle structures and systematic HERFD-XAFS

measurements are necessary.

## References

- (1) Tanuma, S.; Powell, C. J.; Penn, D. R. Calculations of electron inelastic mean free paths for 31 materials. *Surf. Interface Anal.* **1988**, *11*, 577-589.
- (2) Friebel, D.; Miller, D. J.; O'Grady, C. P.; Anniyev, T.; Bargar, J.; Bergmann, U.; Ogasawara, H.; Wikfeldt, K. T.; Pettersson, L. G. M.; Nilsson, A. In situ X-ray probing reveals fingerprints of surface platinum oxide. *Phys. Chem. Chem. Phys.* **2011**, *13*, 262-266.
- (3) Han, B. C.; Miranda, C. R.; Ceder, G. Effect of particle size and surface structure on adsorption of O and OH on platinum nanoparticles: A first-principles study. *Physical Review B* **2008**, *77*, 075410.